J|A|C|S ARTICLES

Published on Web 04/14/2010

Impact of Assembly State on the Defect Tolerance of TMV-Based Light Harvesting Arrays

Rebekah A. Miller, Nicholas Stephanopoulos, Jesse M. McFarland, Andrew S. Rosko, Phillip L. Geissler, and Matthew B. Francis*

Department of Chemistry, University of California, Berkeley, and Materials Sciences Division, Lawrence Berkeley National Laboratories, Berkeley, California 94720-1460

Received November 11, 2009; E-mail: francis@cchem.berkeley.edu

Abstract: Self-assembling, light harvesting arrays of organic chromophores can be templated using the tobacco mosaic virus coat protein (TMVP). The efficiency of energy transfer within systems containing a high ratio of donors to acceptors shows a strong dependence on the TMVP assembly state. Rod and disk assemblies derived from a single stock of chromophore-labeled protein exhibit drastically different levels of energy transfer, with rods significantly outperforming disks. The origin of the superior transfer efficiency was probed through the controlled introduction of photoinactive conjugates into the assemblies. The efficiency of the rods showed a linear dependence on the proportion of deactivated chromophores, suggesting the availability of redundant energy transfer pathways that can circumvent defect sites. Similar disk-based systems were markedly less efficient at all defect levels. To examine these differences further, the brightness of donor-only systems was measured as a function of defect incorporation. In rod assemblies, the photophysical properties of the donor chromophores showed a significant dependence on the number of defects. These differences can be partly attributed to vertical energy transfer events in rods that occur more rapidly than the horizontal transfers in disks. Using these geometries and the previously measured energy transfer rates, computational models were developed to understand this behavior in more detail and to guide the optimization of future systems. These simulations have revealed that significant differences in excited state dissipation rates likely also contribute to the greater efficiency of the rods and that statistical variations in the assembly process play a more minor role.

Introduction

The first step in the photosynthetic process is the collection of sunlight by an array of pigments within the light harvesting (LH) antenna complexes.[1] Through the integration of over 100 chromophores, these centers absorb broad spectrum light with very high efficiency and transfer it to the reaction center. Synthetic mimics of the antenna architecture show great potential for incorporation in solar cells,[2] and as model systems they can provide valuable insight into the ways that energy is transferred and transduced in biological systems. A number of elegant approaches have appeared for the generation of these systems, using both covalent and noncovalent interactions to order multiple chromophores into a functional whole. As an alternative biomimetic approach, recent reports by our laboratory[3] and others[4] have demonstrated that self-assembling proteins, such as the Tobacco Mosaic Virus Coat Protein (TMVP), can serve as scaffolds for the construction of light-harvesting arrays (Figure 1). In these systems, monomers of TMVP bearing a reactive cysteine (from a S123C mutation) are first modified with either a donor (**OG**) or an acceptor (**AF**) chrompohore.[5] The proteins are then combined in various ratios before assembly into either double-layer disks or micrometer-length rods.[6] In the latter case, thousands of chromophores can be positioned in a spiral channel that normally houses the genomic RNA molecule (as shown in Figure 1c). Particular advantages of the protein-based approach include its potential

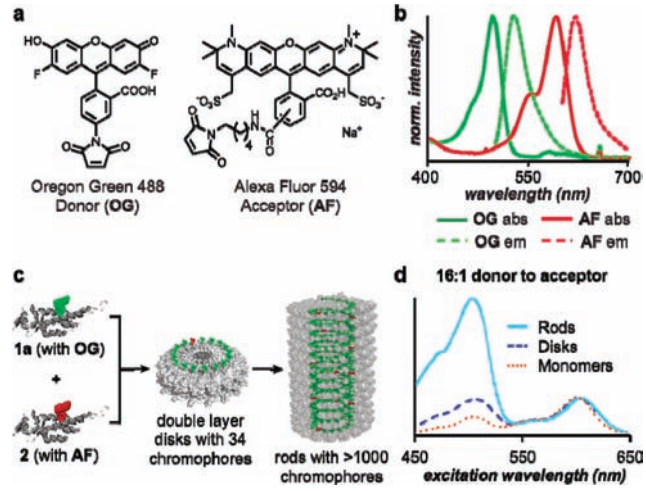

Figure 1. The assembly state of TMVP-based light harvesting systems affects the efficiency of energy transfer. (a) Chemical structures of the donor chromophore (OG) and the acceptor chromophore (AF) used in these studies. (b) Normalized absorption and emission spectra for OG and AF. (c) S123C TMVP monomers labeled with either OG (**1a**) or AF (**2**) were combined and equilibrated under disk- and rod-forming conditions. (d) The donor contribution to acceptor emission is much higher in rod assemblies than in disk assemblies. Emission is monitored at 650 nm, and the spectra are normalized to the acceptor excitation maximum (597 nm).

(1) Nelson, N.; Ben-Shem, A. *Nat. Rev. Mol. Cell Biol.* **2004**, *5*, 971.
(2) Gust, D.; Moore, T. A.; Moore, A. L. *Acc. Chem. Res.* **2001**, *34*, 40.
(3) Miller, R. A.; Presley, A. D.; Francis, M. B. *J. Am. Chem. Soc.* **2007**, *129*, 3104.
(4) Endo, M.; Fujitsuka, M.; Majima, T. *Chem.—Eur. J.* **2007**, *13*, 8660.

10.1021/ja909566z

scalability, environmentally benign production, and synthetic efficiency for the construction of large arrays containing many individual components.

During the development of TMV-based light harvesting systems, the efficiency of energy transfer was found to depend strongly on the assembly state of the protein. For systems with a high ratio of donors to acceptors, rod and disk assemblies derived from a single stock of chromophore-labeled protein exhibited drastically different levels of energy transfer, with rods significantly outperforming disks (Figure 1d). In contrast, disk and rod assemblies showed more similar efficiencies for systems composed of equal amounts of the donor and acceptor. We reasoned that the increased efficiency observed in the high donor rod assemblies may, in part, be due to an inherent tolerance for defects arising from statistical variations, photobleaching, or incomplete protein modification with the chromophores.

To study these important effects, we have developed a new synthetic technique to allow the evaluation of disk- and rod-shaped light harvesting systems containing systematically varied numbers of inactive chromophores. The results reveal that the effectively multidimensional chromophore lattices in rods allow increased transfer rates and introduce redundant energy transfer pathways that allow excitons to circumvent defects better than linear, one-dimensional analogues.[7] In addition, a computational model has suggested that the extended chromophore systems in rods are less susceptible to performance losses due to statistical fluctuations during the assembly process. These studies have also suggested that the rod asemblies possess significantly smaller energy dissipation rates—a feature that is currently unexplained and is the study of ongoing time-resolved experiments. The elucidation of these effects provides functional models that should facilitate the design of more robust light harvesting architectures in the future.

Results and Discussion

An array of chromophores featuring many more donors than acceptors (green and red, respectively, in Figure 2a,b) may require several donor-to-donor resonance energy transfers to shuttle collected energy to the desired destination. This necessity introduces a significant vulnerability to defects, such as bleached or vacant donor sites that can neither absorb light nor transmit excitations. Indeed, time-resolved measurements of photobleaching within the LH2 complex of the natural photosynthetic apparatus indicate that the destruction of a single bacteriochlorophyll within the ring results in complete loss of emission.[8] For this reason biological systems have evolved a variety of intricate mechanisms to prevent and repair photodamage.[9] Lacking an ability to mimic such prophylactic and renewal functions in artificial systems, we have combined experimental and theoretical approaches to explore how the geometry of light-harvesting arrays can be designed to tolerate defects instead.

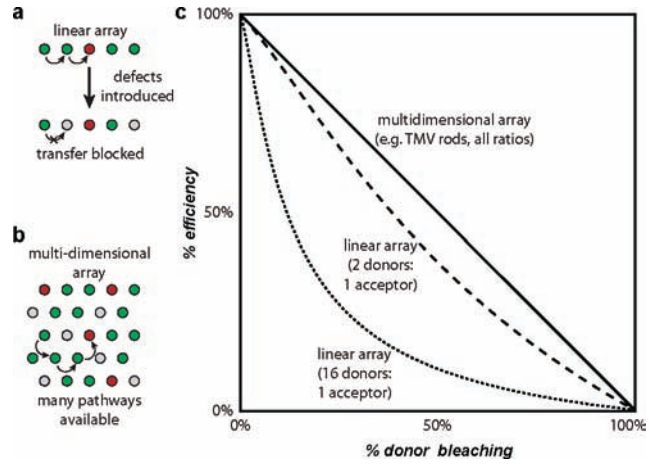

Figure 2. Predicted defect tolerance for linear and two-dimensional light harvesting arrays. (a) In linear or disk arrays, low numbers of defect sites (gray) can block energy transfer from donors (green) to acceptors (red). (b) Multiple transfer pathways are available in multidimensional arrays, which allow defect sites to be circumvented. (c) Mean field approximations predict a linear dependence of overall transfer efficiency on the bleaching level for multidimensional arrays (such as those in TMV rods) at all donor-to-acceptor ratios. For linear arrays, a more rapid decline in efficiency is observed as defects are introduced. This effect is especially pronounced for systems with high donor-to-acceptor ratios.

A linear collection of chrompohores in which transfer can occur principally between adjacent groups, such as the ring of chlorophylls within the LH2 complex, constitutes an effectively one-dimensional array. This geometry generically ensures that defects at a modest fraction of donor sites can greatly compromise efficiency. Within a linear array, any uninterrupted sequence of active donors bounded on either side by defects is corralled; topology prevents radiative energy absorbed by these donors from migrating to an acceptor, as depicted in Figure 2a. The prevalence of such corrals increases sharply with the fraction x of donors that are defective. Specifically, for an infinite chain of chromophores, whose donors and acceptors are arranged at random, the population of active donors rendered unproductive in this way grows as

$$[xf/(1 - f(1 - x))]^2 \qquad (1)$$

where f is the fraction of chromophore sites occupied by donors (both active and inactive). The correspondingly faster-than-linear decay of overall light-harvesting efficiency (neglecting dissipation of excitations on active donors through emission or thermal relaxation pathways) is plotted in Figure 2c for the two values of f studied in our experiments.

(5) For other examples of chromophore labeled viruses, see: (a) Wang, Q.; Lin, T.; Tang, L.; Johnson, J. E.; Finn, M. G. *Angew. Chem., Int. Ed.* **2002**, *41*, 459–462. (b) Demir, M.; Stowell, M. H. B. *Nanotechnology* **2002**, *13*, 541. (c) Schlick, T. L.; Ding, Z. B.; Kovacs, E. W.; Francis, M. B. *J. Am. Chem. Soc.* **2005**, *127*, 3718–3723. (d) Kovacs, E. W.; Hooker, J. M.; Romanini, D. W.; Holder, P. G.; Berry, K. E.; Francis, M. B. *Bioconjugate Chem.* **2007**, *18*, 1140–1147. (e) Endo, M.; Wang, H.; Fujitsuka, M.; Majima, T. *Chem.—Eur. J.* **2006**, *12*, 3735–3740. (f) Barnhill, H. N.; Reuther, R.; Ferguson, P. L.; Dreher, T.; Wang, Q. *Bioconjugate Chem.* **2007**, *18*, 852–859. (g) Xie, F.; Sivakumar, K.; Zeng, Q.; Bruckman, M. A.; Hodges, B.; Wang, Q. *Tetrahedron* **2008**, *64*, 2906–2914. (h) Steinmetz, N. F.; Bize, A.; Findlay, K. C.; Lomonossoff, G. P.; Manchester, M.; Evans, D. J.; Prangishvili, D. *Adv. Funct. Mater.* **2008**, *18*, 3478–3486. (i) Stephanopoulos, N.; Carrico, Z. M.; Francis, M. B. *Angew. Chem., Int. Ed.* **2009**, *48*, 9498–9502.

(6) For the specific buffer conditions leading to these different assembly states, see the Supporting Information of this paper and of ref 3.

(7) For examples of natural systems that use three-dimensional chromophore assemblies for a similar advantage, see: (a) Sener, M. K.; Lu, D.; Ritz, T.; Park, S.; Fromme, P.; Schulten, K. *J. Phys. Chem. B* **2002**, *106*, 7948–7960. (b) Yang, M.; Damjanovic, A.; Vaswani, H. M.; Fleming, G. R. *Biophys. J.* **2003**, *85*, 140–158. (c) Sener, M. K.; Park, S.; Lu, D. Y.; Damjanovic, A.; Ritz, T.; Fromme, P.; Schulten, K. *J. Chem. Phys.* **2004**, *120*, 11183–11195. (d) Vasil'ev, S.; Bruce, D. *Plant Cell* **2004**, *16*, 3059–3068. (e) Sener, M. K.; Jolley, C.; Ben-Shem, A.; Fromme, P.; Nelson, N.; Croce, R.; Schulten, K. *Biophys. J.* **2005**, *89*, 1630–1642.

(8) Bopp, M. A.; Jia, Y.; Li, L.; Cogdell, R. J.; Hochstrasser, R. M. *Proc. Natl. Acad. Sci. U.S.A.* **1997**, *94*, 10630.

(9) (a) Niyogi, K. *Ann. Rev. Plant Phys.* **1999**, *50*, 333. (b) Niyogi, K. *Curr. Opin. Plant Biol.* **2000**, *3*, 455.

Multidimensional arrays, by contrast, feature highly redundant transfer pathways connecting any two sites. Corrals therefore occur appreciably only at high defect fraction x. To the extent that connectivity is no longer an issue (and again neglecting dissipation), efficiency will decay simply as $1 - x$, reflecting only the attrition of functional light-absorbing groups. As shown in Figure 2c, this result holds independent of donor/acceptor composition. A simple accounting for the effects of dissipation rate changes the slope of this decay and its dependence on f, but not its linear nature.

Inspired by this expected performance improvement, we therefore set out to construct TMVP-templated light harvesting systems in which energy can transfer both parallel and perpendicular to the rod's axis and then characterize their defect tolerance by varying the proportion of monomers that lacked active chromophore groups.

Generation of Light Harvesting Systems Containing Controlled Numbers of Defect Sites. Our first approach to building defect-containing arrays was simply to coassemble mixtures of monomers bearing and lacking chromophore groups. Unmodified monomers were combined in various ratios with monomers labeled with the OG donor dye (**1a**) and allowed to equilibrate under rod forming conditions (acetate buffer, pH 5.5).[10] However, size exclusion chromatography revealed that samples containing greater amounts of unmodified protein assembled less readily (Supporting Information, Figure S1). In addition, a comparison of the absorbance spectra for assembled rods and the remaining monomer aggregates within each sample indicated that the unmodified protein was excluded in favor of chromophore-labeled protein. In contrast, previous studies on the coassembly of donor and acceptor-labeled TMVP (**1a** and **2**, respectively) showed that the two conjugates assembled with similar efficiencies. We suspect that the enhanced assembly of chromophore-labeled TMPV arises because of favorable interactions that mimic those involving the aromatic RNA bases, although we do not have any direct evidence for this at this time. For the purposes of these experiments, however, the differential assembly characteristics of unmodified and modified TMVP prevented the use of this strategy.

We next explored the chemical deactivation of the chromophores as a means to prohibit energy transfer while conserving their general aromatic structures. This approach would then enable the incorporation of "bleached" and unbleached chromophore−TMVP conjugates into rods with similar efficiencies. Previous studies of fluorophore bleaching have reported the use of small molecule reductants, such as tris(2-carboxyethyl)phosphine (TCEP), sodium dithionite, and sodium borohydride ($NaBH_4$), as well as epitope quenching and electrochemical methods.[11] As many of these reagents would also be expected to react with the maleimide portion of the dyes required for protein attachment, these steps needed to be carried out after the cysteine alkylation step. However, the applicability of these methods for the reductive bleaching of chromophores attached to proteins has not been established.

A number of reagents were screened for the reduction of TMVP conjugates labeled with OG, including several borohydrides and silanes (Figure 3). Of these, only exposure to $NaBH_4$ reduced the absorbance and emission of **1a**. The reaction was not ideal for the protein, however, as it resulted in significant foaming and changes in the pH that led to sample loss.

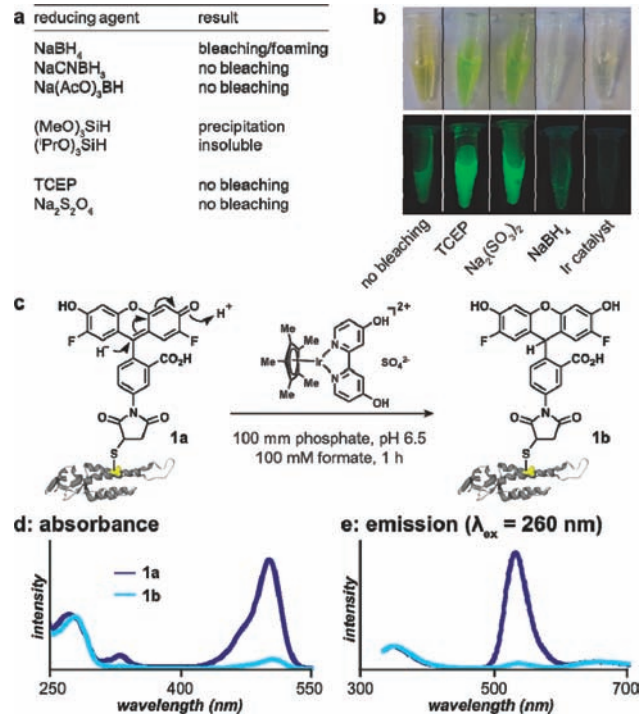

Figure 3. Chemical bleaching of chromophore-modified TMVP. (a) Several reductants were added to a solution of free dye in "monomer" buffer. (b) Visualization of OG absorbance (top) and emission (bottom) indicated only two successful reactions. (c) The proposed mechanism of Ir-catalyzed bleaching involves a hydride attack on the chromophore, followed by protonation. (d) Absorbance and (e) emission spectra of the protein conjugate before (**1a**) and after (**1b**) reduction. Spectra were normalized by protein concentration, as monitored by tryptophan emission at 330 nm (ex. 290 nm).

Due to the drawbacks associated with treatment with $NaBH_4$, an improved bleaching method was developed. A water-soluble iridium(III) complex is known to act as a reducing agent in the presence of buffered formate ions,[12] and we have previously reported the use of a related species for the reductive alkylation of lysine residues on proteins.[13] The reduction is mild and rapid, occurring at pH 7.4 in aqueous buffer. Exposure of **1a** to a related catalyst ([Cp*Ir(4,4′-dihydroxy-2,2′-bipyridine)-(H_2O)]SO_4,[14] **3**) in the presence of buffered formate ion as a stoichiometric hydride source eliminated the chromophore absorbance and emission in under 1 h (Figure 3c). No protein precipitation was observed. Size exclusion chromatography of **1b** confirmed a >90% loss of the absorbance and emission after bleaching (Figure 3d,e).

To confirm that the Ir-catalyzed bleaching occurred through reduction of the chromophore, high resolution mass spectrometry was used (Figure 4a). Prior to bleaching, three primary protein species were observed, corresponding **1a** (17971 amu), a maleimide hydrolysis product (17989 amu), and a previously

(10) (a) Klug, A. *Philos. Trans. R. Soc. London, Ser. B* **1999**, *354*, 531. (b) Butler, P. J. G. *Philos. Trans. R. Soc. London, Ser. B* **1999**, *354*, 537.
(11) (a) Kinsey, B. M.; Kassis, A. I.; Fayad, F.; Layne, W. W.; Adelstein, S. J. *J. Med. Chem.* **1987**, *30*, 1757. (b) Compton, R. G.; Mason, D.; Unwin, P. R. *J. Chem. Soc., Faraday Trans. 1* **1988**, *84*, 483. (c) Kranz, D. M.; Voss, E. W., Jr. *Mol. Immunol.* **1981**, *18*, 889.
(12) (a) Abura, T.; Ogo, S.; Watanabe, Y.; Fukuzumi, S. *J. Am. Chem. Soc.* **2003**, *125*, 4149. (b) Himeda, Y.; Onozawa-Komatsuzaki, N.; Miyazawa, S.; Sugihara, H.; Hirose, T.; Kasuga, K. *Chem.—Eur. J.* **2008**, *14*, 11076.
(13) McFarland, J. M.; Francis, M. B. *J. Am. Chem. Soc.* **2005**, *127*, 13490.
(14) Himeda, Y.; Onozawa-Komatsuzaki, N.; Sugihara, H.; Kasuga, K. *Organometallics* **2007**, *26*, 702.

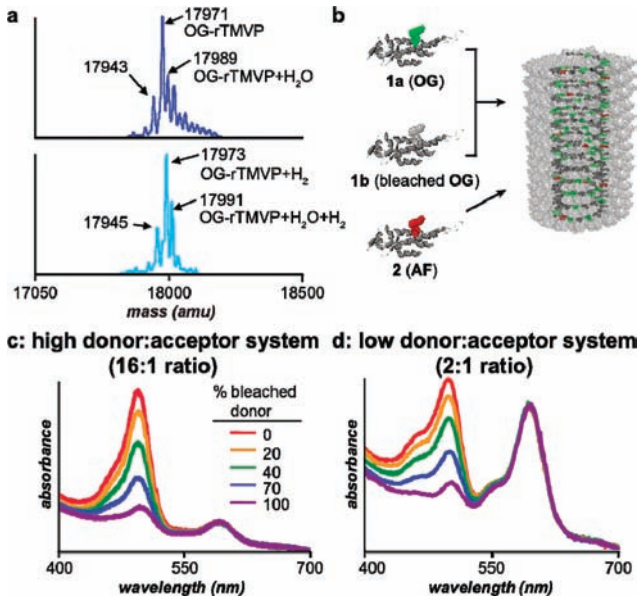

Figure 4. Construction of light-harvesting arrays containing varying levels of "bleached" donor chromphores. (a) ESI mass spectra comparing the OG-modified TMVP before (top) and after (bottom) exposure to the iridium-mediated reduction. (b) The overall level of bleaching was established by combining varying levels of **1a** with **1b**, while the relative amount of **2** remained constant. Absorbance measurements showed a decrease in donor absorbance for (c) a 16:1 ratio of **1** to **2** and (d) a 2:1 ratio of **1** to **2**.

observed side product arising during protein expression (also labeled with OG maleimide: 17943 amu). The reconstructed mass of each species increased by two mass units following reduction, equivalent to the addition of H_2. The substrate scope of the catalyst was investigated by testing the reduction of several related chromophores. In each case, complete bleaching occurred in less than 45 min (Supporting Information, Figure S5). Thus, the Ir-catalyst will likely be useful in future studies investigating the response of TMV-based LH systems to acceptor bleaching as well.

Effects of Defect Sites on Energy Transfer Efficiency. The development of this method allowed the investigation of the defect tolerance of disks and rods. Three stock solutions of monomeric **1a**, **1b**, and **2** were prepared. The concentration of each solution was determined using the Bradford assay,[15] after which they were combined in various ratios for assembly (Figure 4b). To represent a system containing a high number of donors, the efficiency of energy transfer was monitored in disk and rod assemblies containing a 16:1 donor to acceptor ratio. The number of defects was controlled by substituting **1a** monomers with the photoinactive **1b** monomers before assembly. The level of **2** was held constant throughout. Following assembly, the presence of rods or disks was confirmed using size exclusion chromatography. UV−vis measurements revealed that the absorbance of OG decreased with increasing amounts of **1b**, as expected (Figure 4c,d).

To determine the effect of donor inactivation on energy transfer, the overall efficiency of each light harvesting system was measured by comparing the excitation spectra to the absorbance spectra,[16,17] normalized at the acceptor wavelength

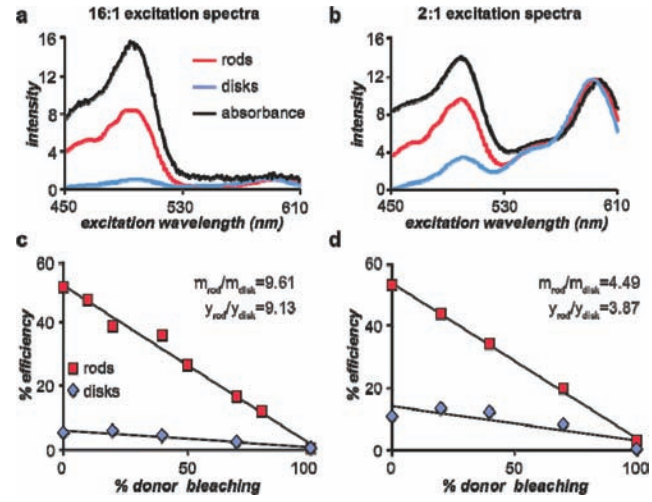

Figure 5. A comparison of the efficiencies of rod and disk assemblies containing (a) 16 donors per acceptor or (b) 2 donors per acceptor. Excitation spectra indicate the donor contribution to acceptor emission (measured at 615 nm) and are overlaid with the absorbance spectrum for each system. The dependence of the efficiency on donor bleaching in disk and rod assemblies is shown for both (c) high- and (d) low-donor systems. The data were fit using a linear trendline to obtain numerical values representing this dependence.

(597 nm). The excitation spectra for all systems converged at 100% donor bleaching to an identical profile, which was termed 0% efficiency and was subtracted from all spectra before analysis (full excitation spectra corresponding to this experiment appear in Supporting Information, Figure S6). Rods exhibited reasonable energy transfer in the unbleached system (∼52% efficiency) that was diminished with the inclusion of defects (Figure 5a and c, red traces and data points). Disk assemblies with a 16:1 donor to acceptor ratio were much less efficient even before defect incorporation, with only 5% efficiencies measured (Figure 5a and c, light blue).

The efficiency of energy transfer in rods containing a 2:1 ratio of **1a** to **2** was similar to that of the 16:1 system (∼53%). A similar linear decrease was observed with increasing levels of defects (Figure 5b and d, red). In this system, complete removal of the donor chromophores reduced the experimentally measured energy transfer efficiency to ∼3% (Supporting Information, Figure S7). The efficiency of defect-free disks (∼11%) containing a 2:1 ratio of **1a** to **2** was lower than that for 2:1 rods but higher than that of the 16:1 disk system (Figure 4b and d, light blue).

Effects of Assembly State on Transfer Efficiency. A linear dependence of overall efficiency on the defect fraction can be seen in both Figures 2c and 5c,d, providing strong evidence for the ability of the extended "two-dimensional" chromophore arrays in rods to participate in multiple energy transfer pathways. The data were less clear for the double-disk arrays, as they were consistently less efficient at virtually all defect fractions. Furthermore, the assembly state of TMVP affected energy transfer efficiency to a much greater degree in the high donor systems. In the 16:1 donor to acceptor system, unbleached rods were over 9 times more efficient than disks, whereas in the 2:1 donor to acceptor system the rods were only approximately 4 times more efficient. In addition, the superior energy transfer efficiencies exhibited by rod assemblies were significantly

(15) Bradford, M. *Anal. Biochem.* **1976**, *72*, 248.
(16) Chen, M.; Ghiggino, K. P.; Thang, S. H.; Wilson, G. J. *Angew. Chem., Int. Ed.* **2005**, *44*, 4368–4372. (b) Bai, F.; Chang, C. H.; Webber, S. E. *Macromolecules* **1986**, *19*, 2484–2494. (c) Gomez, R.; Segura, J. L.; Martin, N. *Org. Lett.* **2005**, *7*, 717–720.
(17) Dale, R. E.; Eisinger, J.; Blumberg, W. E. *Biophys. J.* **1979**, *26*, 161–193.

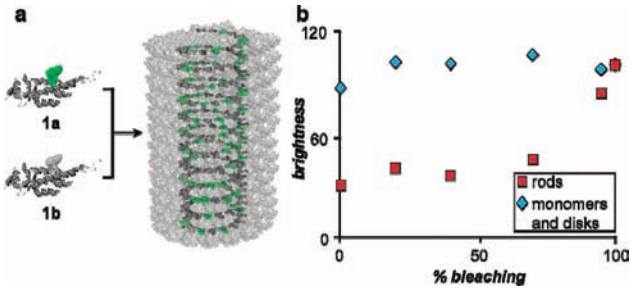

Figure 6. The brightness of chromphores in assemblies containing only bleached and unbleached donors. (a) All systems are constructed by combining stoichiometric ratios of **1a** and **1b** before assembly. (b) The brightness of the donor chromphore is determined as a function of bleaching for rods and an equilibrating mixture of disks and monomers. To allow direct comparison, the two data sets are normalized to 100% brightness at 100% bleaching.

reduced as defects were introduced, whereas bleaching affected energy transfer efficiency in disk assemblies to a much lesser degree. This suggested that the cylindrical two-dimensional array of donor chromophores within the TMVP rods possesses an inherent property that enhances energy transfer; this property is clearly absent from disk assemblies.

The presence of an increased number of donor-to-donor transfer pathways in rods should manifest as a difference in the donor (**1a**) emission lifetime and/or quantum yield. Previous time-resolved studies support this claim, with donor-to-donor transfer on the picosecond scale contributing to the decay of OG emission intensity.[18] To confirm the presence of donor−donor transfers further, donor-only systems were assembled using 0−100% **1b** (Figure 6a). The brightness, defined as the fluorescence emission normalized by chromophore absorbance, was measured as a function of the degree of defect incorporation (Figure 6b). The brightness of intact chromophores in monomer and disk assemblies was not affected by the presence of the bleached chromophores, suggesting that a limited number of donor-to-donor transfer pathways occur in these systems. In contrast, the brightness of intact chromophores increased by almost 3-fold in rods containing 95% defects, compared to defect-free rods.

These data suggest that donor-to-donor transfer is significantly enhanced in rods (compared to disks), and the linear dependence of acceptor emission on donor bleaching indicates that extended donor-to-donor pathways are crucial in funneling the energy to the acceptor chromophores with high efficiency. Because the chromophore composition is identical in the two assembly states, the difference in donor transfer ability is best attributed to their geometrical arrangement. Energy transfer in disks is expected to occur horizontally along the plane of the disk, whereas, in rods, both horizontal and vertical transfers can occur. Thus, the vertical transfer appears to be a key reason for the increased efficiency in rods.

To explore this possibility, the location and orientation of the donor chromophore within the protein matrix were estimated based on the void space normally occupied by the RNA genome and the topology of the protein surface (Figure 7a,b). The optimized arrangement shows the xanthene core of the chromophores oriented vertically with respect to the rod axis, indicating that the dipole moment of the chromophore favors vertical transfer (Figure 7c). The relative rates of energy transfer

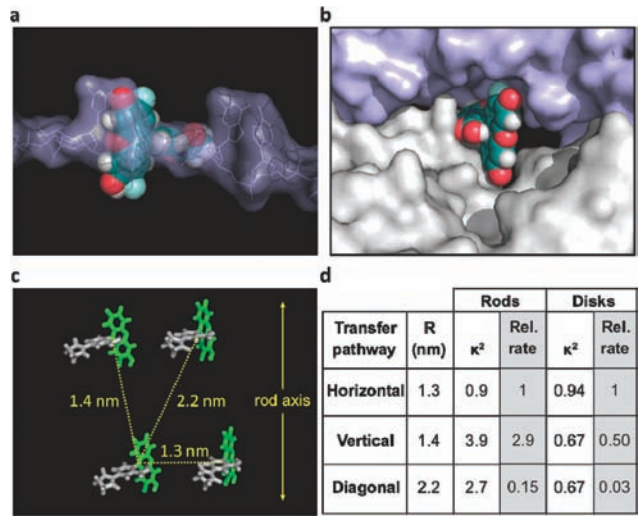

		Rods		Disks	
Transfer pathway	R (nm)	κ^2	Rel. rate	κ^2	Rel. rate
Horizontal	1.3	0.9	1	0.94	1
Vertical	1.4	3.9	2.9	0.67	0.50
Diagonal	2.2	2.7	0.15	0.67	0.03

Figure 7. Analysis of the chromophore orientation within TMV rods. A model predicting the arrangement of chromophores within the protein assembly was developed based on fitting the chromphore (a) within the void space left by the absence of RNA and (b) within the protein contours. (c) The optimized arrangement suggests that the xanthene cores of the donor chromophores are held parallel to the rod axis, aligning the dipole moment for transfer in the vertical direction. (d) The rates of transfer in the vertical and diagonal directions were calculated relative to that in the horizontal direction, taking into account the distance and orientation of the chromophores. Chromphore orientation can be described by the orientation factor κ^2, where $\kappa^2 = (\cos\theta_T - 3\cos\theta_D \cos\theta_A)$ and θ_T is the angle between the donor and acceptor chromophores (see Supporting Information).[17]

in the horizontal, vertical, and diagonal directions were calculated taking into account the distance and orientation of the chromophores (Figure 7d), leading to the conclusion that vertical transfer occurs around 3 times as fast as horizontal transfer. Comparatively, diagonal transfer is negligible. In disks, where the top layer of chromophores is not embedded in the protein, it is more likely that a random orientation ($\kappa = 2/3$) is involved in the vertical and diagonal interactions. For randomly oriented chromophores, the Förster radius was previously estimated to be 4.0 nm for transfer between two molecules of chromophore **1** and 4.4 nm for transfer between chromophores **1** and **2**.[3] This should further reduce the transfer rates. In rods, we are currently using polarized spectroscopy techniques to confirm the orientation of the donors relative to the long axis.

Development of a Model to Simulate Energy Transfer. To investigate the differences in energy transfer within disks and rods further, we have developed and numerically simulated a simple model for energy transfer in an arbitrarily ordered network of chromophores. We represented the chromophores as a helical array of lattice sites, each occupied either by a donor or by an acceptor. One helical turn in this model comprises 17 lattice sites, matching the periodicity of natural TMV capsids. Double-layer disks were modeled as a system containing 34 such sites, whereas rods were modeled using 5000 sites. Each site was randomly assigned its identity (either D or A) given an input donor fraction. A certain fraction of donors was then assigned as "bleached".

Energy transfer trajectories were propagated stochastically with a kinetic Monte Carlo algorithm, in which events are selected with probabilities proportional to their rates. Each simulation began with the excitation of a randomly chosen donor and, assuming no bleaching, tracked the fate of that photon until it either reached an acceptor or was dissipated by thermal relaxation or fluorescence emission. For a given donor, the

(18) (a) Ma, Y.-Z.; Miller, R. A.; Fleming, G. R.; Francis, M. B. *J. Phys. Chem. B* **2008**, *112*, 6887–6892. (b) Pearlstein, R. M.; Hemenger, R. P. *Proc. Natl. Acad. Sci. U.S.A.* **1978**, *75*, 4920.

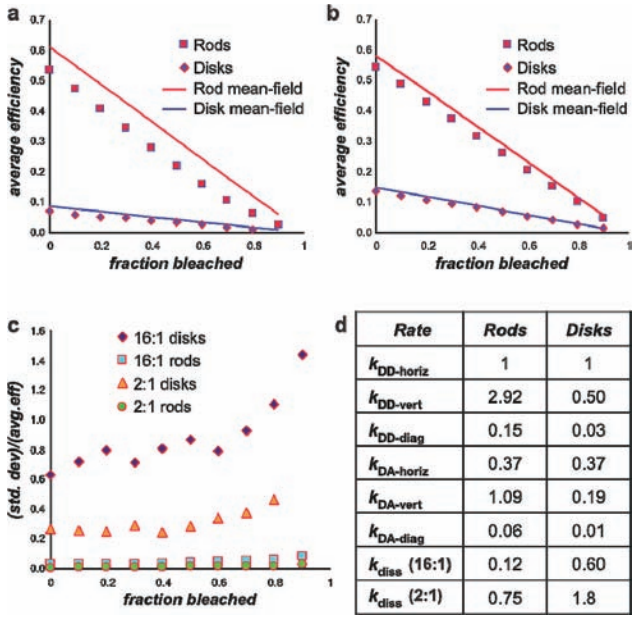

Rate	Rods	Disks
$k_{DD\text{-}horiz}$	1	1
$k_{DD\text{-}vert}$	2.92	0.50
$k_{DD\text{-}diag}$	0.15	0.03
$k_{DA\text{-}horiz}$	0.37	0.37
$k_{DA\text{-}vert}$	1.09	0.19
$k_{DA\text{-}diag}$	0.06	0.01
k_{diss} (16:1)	0.12	0.60
k_{diss} (2:1)	0.75	1.8

Figure 8. Results from the computational simulation indicating the efficiency vs bleached fraction for (a) the 16:1 system and (b) the 2:1 system. The points indicate the simulation results, while the lines indicate the predicted efficiencies from the mean-field model. (c) The standard deviation of the systems, normalized by the average efficiency, as a function of bleached fraction indicates that disks have a much greater variability in efficiency than rods, and the variability increases with the fraction of donors bleached. (d) The relative rate constants of energy transfer between donors (D) and acceptors (A), were derived from Figure 7 and the previously reported energy transfer rates (see Supporting Information).

excitation was transferred or dissipated depending on the identity of its eight immediate neighbors and the relative energy transfer rates between them (see Supporting Information for a complete description of the model). Due to the alignment of chromophore groups relative to the helical axis, we expect rates of energy transfer among adjacent sites to depend on direction as well as on the species involved. The complete set of rate constants used for our numerical simulations, both for transfer and for dissipation, are presented in Figure 8. The relative energy transfer rates were estimated from the time-dependent measurements determined previously[18a] and the relative orientation of the chromophores depicted in Figure 7.

Illustrative analytical estimates of efficiency can be obtained from a mean field approximation that neglects spatial variations in the local populations of active donors, acceptors, and defects. Here we take the probability that any excited donor transfers energy directly to an acceptor to be determined simply by the rod's overall composition and rate constants for energy transfer and dissipation. In this model, which neglects the specific arrangement of donors and acceptors around a given site, the probability, P, that a given excitation reaches an acceptor (possibly via multiple donor-to-donor transfers) is

$$P = (1 - f)\alpha/[1 + (1 - f)\alpha] \quad (2)$$

This result is independent of donor-to-donor transfer kinetics, involving only the ratio of rates for single-step donor-to-acceptor transfer and for dissipation:

$$\alpha = (Z_{horiz}k_{DA\text{-}horiz} + Z_{vert}k_{DA\text{-}vert} + Z_{diag}k_{DA\text{-}diag})/k_{diss} \quad (3)$$

where Z_{horiz} is the number of nearest horizontal neighbors adjacent to a given lattice site (= 2 for both disks and rods), Z_{vert} is the number of vertical neighbors (= 2 for rods and 1 for disks), and Z_{diag} is the number of diagonal neighbors (= 4 for rods and 2 for disks). The three k_{DA} rate constants govern the kinetics for energy transfer from donor to acceptor in the given direction (horizontal, vertical, or diagonal), and k_{diss} is the rate constant for loss of the excitation through dissipative channels. Note that this result, which is quite accurate for both rods and disks (see lines in Figure 8a,b), is independent of the defect fraction x, so that the degradation of efficiency with bleaching remains linear, as noted above.

All four systems investigated in this paper were simulated (disks and rods at both 16:1 and 2:1 donor/acceptor ratios). For each run a total of 100 000 photons were tracked, and each simulation was run 100 times for a given donor/acceptor ratio and defect fraction. The efficiency of each run was defined as the fraction of photons that were able to reach the acceptor in a given simulation.

Much like the experimental data, the simulations show a linear decrease in efficiency with an increased bleach fraction, Figure 8a,b. However, these models point to another difference between these systems. To fit the absolute efficiency values, the rods must have a suppressed overall dissipation rate (k_{diss}), relative to the donor−acceptor transfer rates (Figure 8d). Considering that half of the chromophores in the double-disk assemblies are exposed to the aqueous buffer and should be more free to rotate and potentially contact-quench, this is a reasonable assumption. To verify this hypothesis, we are currently working to determine the magnitude and origin of these dissipation rates using time-resolved techniques.

The results of these simulations also reveal that statistical fluctuations in the assembly process play a minor but detectable effect on the efficiency that can be achieved. In the disks, which have only 34 monomers, a much greater variability is observed in their composition. A 16:1 disk has a significant chance of having no acceptors (in which case the light harvesting efficiency will be zero). Furthermore, as the defect fraction increases, the disks are more likely to have donors that are isolated from any available acceptors. The rods, on the other hand, have 5000 units and thus behave much more like a "bulk" material that is less sensitive to fluctuations in composition due to defective sites. The effect of this intrinsic heterogeneity in the disks can be seen in Figure 8c, which plots the standard deviation in efficiency (relative to the mean) for the 100 runs performed for each bleach fraction. In all cases, the disk samples have greater variation than the rods.

Conclusions

Our ability to introduce a controlled number of defects into TMVP-templated light harvesting arrays has yielded insight into the superior energy transfer efficiencies observed in rod assemblies. For the high donor systems, rods exhibited markedly higher efficiencies than disks, but this superiority was dependent on the degree of donor "bleaching". In addition, the photophysical properties of donor chromophores depended on the degree of bleaching only in rod assemblies. Together, these data suggest that the enhanced light harvesting in rod systems is due to the presence of extended donor-to-donor transfer pathways. Furthermore, structural modeling and Förster analysis suggest that vertical transfer occurs more rapidly than horizontal transfer due to the orientation of the chromophores within the protein matrix. The natural photosynthetic system has optimized both chromophore distances and their orientations to control the rate and direction of energy transfer.[19] The development of this

methodology for examining the impact of orientation in synthetic systems shows that the TMVP-templated systems are one of the first synthetic light harvesting systems to display this behavior.

Finally, the statistical variation in the smaller assemblies was shown to be negligible in rods at all defect levels, indicating an inherent additional advantage of building extended three-dimensional systems. Current efforts are underway to refine the simulations with a more accurate description of the energy transfer processes to predict the performance of future systems before they are built. These models will also be used to guide the selection of photocatalytic groups that can use the absorbed energy to drive chemical reactions.

(19) (a) Freer, A.; Prince, S.; Sauer, K.; Papiz, M.; Lawless, A. H.; McDermott, G.; Cogdell, R.; Isaacs, N. W. *Structure* **1996**, *4*, 449. (b) Philipson, K. D.; Sauer, K. *Biochemistry* **1972**, *11*, 1880. (c) Simonetto, R.; Crimi, M.; Sandona, D.; Croce, R.; Cinque, G.; Breton, J.; Bassi, R. *Biochemistry* **1999**, *38*, 12974.

Supporting Information Available: Full synthetic procedures, a description of the modeling techniques, and the spectral data used to generate the curves in Figure 5 are provided. This material is available free of charge via the Internet at http://pubs.acs.org.

Acknowledgment. This work was supported by the Director, Office of Science, Materials Sciences and Engineering Division, of the U.S. Department of Energy under Contract No. DE-AC02-05CH11231. We gratefully acknowledge the Berkeley Chemical Biology Graduate Program (NRSA Training Grant 1 T32 GMO66698) for generous financial support. R.A.M. acknowledges the NSF IGERT program (DGE-0333455) for a graduate fellowship. We would also like to thank Prof. Kenneth H. Sauer for many helpful discussions.

JA909566Z